

- Liepmann, H. W., Roshko, A. & Dhawan, S. 1949 On the reflection of shock waves from boundary layers. Galt Report (Pasadena, Cal.), or *Tech. Memor. Nat. Adv. Comm. Aero., Wash.*, no. 2334 (1951).
- Lighthill, M. J. 1945 *Rep. Memor. Aero. Res. Council., Lond.*, no. 2112.
- Lighthill, M. J. 1950 *Quart. J. Mech.* 3, 303.
- Lighthill, M. J. 1953 *Proc. Roy. Soc. A*, (part II). (In the press.)
- Mair, W. A. 1952 *Phil. Mag.* 43, 695.
- Oswatitsch, K. & Wieghardt, K. 1941 German wartime report, reprinted as *Tech. Memor. Nat. Adv. Comm. Aero., Wash.*, no. 1189 (1948).
- Robinson, A. 1950 *Coll. Aero. Rep.* no. 37 (Cranfield).
- Rubach, H. L. 1913 Dissertation (Göttingen).
- Stewartson, K. 1949 *Proc. Roy. Soc. A*, 200, 84.
- Stewartson, K. 1951 *Proc. Camb. Phil. Soc.* 47, 545.
- Tsien, H. S. & Finston, M. 1949 *J. Aero. Sci.* 16, 515.

Cross-section for the photodisintegration of carbon into three α -particles

BY F. K. GOWARD AND J. J. WILKINS

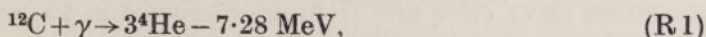
Atomic Energy Research Establishment, Harwell, Didcot, Berkshire

(Communicated by Sir John Cockcroft, F.R.S.—Received 25 November 1952—
Revised 14 January 1953)

The cross-section for the photodisintegration $^{12}\text{C}(\gamma, 3\alpha)$ has been determined for γ -ray energies up to about 60 MeV from a study of 2500 stars in nuclear emulsions. The methods used in selecting and identifying the stars are described, and full details are given of the corrections (for escape, observer efficiency, etc.) required for converting the experimental data into cross-section values. The cross-section exhibits at least five resonances, situated at γ -ray energies (E_γ) of 17.3, 18.3, 21.9, 24.3 and 29.4 MeV, and a strong minimum at $E_\gamma \sim 20.5$ MeV. This behaviour suggests that a well-defined compound nucleus is formed, the minimum near 20.5 MeV resulting from (γ, n) and (γ, p) competition. Furthermore, the finer details of the cross-section data are consistent with current knowledge of the ^{12}C level structure. The integrated cross-section is 1.21 ± 0.16 MeV mb for $E_\gamma < 20.5$ MeV, a further 2.8 ± 0.4 MeV mb for $20.5 \leq E_\gamma < 42$ MeV, and < 0.2 MeV mb for $42 \leq E_\gamma < 60$ MeV (where the symbol mb denotes 10^{-27} cm²). As a subsidiary result of the main work, the existence of the reaction $^{13}\text{C}(\gamma, n) 3\alpha$ has been established.

1. INTRODUCTION

By irradiating nuclear emulsions with γ -rays produced by the proton bombardment of lithium it has been possible to establish the reaction



and to study some of its properties (Hänni, Telegdi & Zünti 1948; Wäffler & Younis 1949; Telegdi & Zünti 1950; Nabholz, Stoll & Wäffler 1951, 1952; Chastel 1951; Glätti, Seipel & Stoll 1952). Characteristic three-track stars are formed in the emulsions, the majority resulting from the 17.6 MeV γ -rays and a small proportion from the 14.6 MeV γ -rays. The experiments have been limited by the

restricted range of γ -ray energies provided by this source, and by the poor geometrical arrangements made necessary by the low γ -ray intensities available.

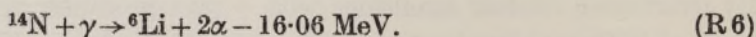
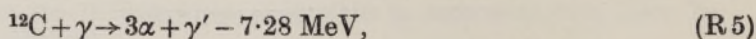
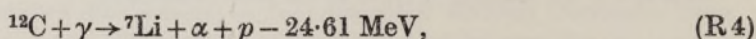
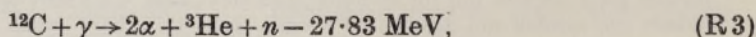
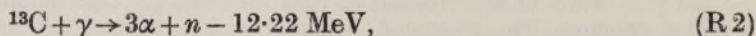
In order to overcome these limitations, Ilford E1 and C2 emulsions have been irradiated with synchrotron bremsstrahlung of 21, 23 to 28, 33 and 70 MeV peak energy. The intensity produced by a synchrotron enables adequate exposures to be made in a few minutes with good geometry (at a metre or so from the target), and the cross-section may be studied over a wide and continuous range of energies. The variation of cross-section with energy is calculable from the results of a single irradiation, if the bremsstrahlung spectrum is known, by applying to each star the equation

$$E_{\gamma} = E_T + E_B, \quad (1)$$

where E_{γ} is the energy of the particular γ -ray quantum forming the star, E_T is the total kinetic energy of the three α -particles, and E_B is the mass threshold energy, 7.28 MeV, deduced from the data of Li, Whaling, Fowler & Lauritsen (1951). The method gives much higher resolution (better than 1.0 MeV) than that generally achieved in measurements of photodisintegration cross-sections, where an analysis is made of a yield curve obtained by varying the peak energy of the bremsstrahlung.

Some further irradiations have also been carried out with lithium γ -rays, mainly to obtain data required for an analysis of the energy and momentum resolution given by nuclear emulsions (Wilkins 1952). In the present paper the $^{13}\text{C}(\gamma, 3\alpha)$ results obtained, together with the more extensive results of Nabholz *et al.* (1952), are correlated with the bremsstrahlung work in order to study the $^{13}\text{C}(\gamma, 3\alpha)$ cross-section variation more closely near 17.6 MeV.

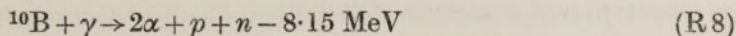
The high energies used in the present experiments raise problems of star identification not generally met with when using lithium γ -rays. Up to 20 MeV, reaction (R 1) is the only effective star-producing reaction in non-loaded emulsions, but at higher energies many other reactions become energetically possible and may cause confusion. A comprehensive list would be of prohibitive length, but typical examples of reactions giving three-track stars are



Reactions (R 2), (R 3) and (R 5) are discussed in §3; reactions (R 4) and (R 6) are already known to occur (Brinkworth, Goward & Wilkins 1952; Wilkins & Goward 1950). Many four-track stars are also possible, but they may be confused with three-track stars if one track is short or obscured. This is especially likely in the reaction (Goward & Wilkins 1952*b*)



A further factor in the present experiments is that borax-loaded emulsions were used in obtaining about half the total data, in order to enable reactions in ^{10}B and ^{11}B to be studied at the same time. The known boron reactions (Goward, Titterton & Wilkins 1950), of which



is by far the most prolific, must therefore be added to the foregoing list. Finally, a similar list of fast neutron reactions must be considered, of which the $^{12}\text{C}(n, n) 3\alpha$ reaction is an example (Green & Gibson 1949). Some fast neutrons would be expected to accompany the bremsstrahlung beam.

In the types of emulsion used, an experienced observer can usually, by inspection, distinguish protons, deuterons and tritons, as a class, from α -particles and heavier nuclei. The usual grain counting and multiple-scattering techniques are of little assistance because of the shortness of the tracks. A more powerful method of star identification is therefore required, and is provided by the use of a momentum-balance criterion (§ 3(b)). The method must be developed in a proper statistical manner (Goward & Wilkins 1950; Wilkins 1952) to yield valid results. In the present experiments, study of reaction (R 1) at energies below 20 MeV is used to establish the momentum-balance techniques necessary for work at higher energies and for the identification of other reactions.

Analysis of the selected $^{12}\text{C}(\gamma, 3\alpha)$ stars falls naturally into two parts. First, the cross-section for the $^{12}\text{C}(\gamma, 3\alpha)$ reaction, (R 1), has been evaluated and forms the subject of the present paper. Secondly, the mechanism by which the reaction proceeds, and the information it gives about the ^{12}C and ^8Be nuclei, is being evaluated and will be described later. Some preliminary results on both parts of the analysis have already been published in condensed form. The abrupt fall and subsequent re-increase of the cross-section and some associated changes in mechanism have been reported (Goward & Wilkins 1951*b*; Wilkins & Goward 1951), and confirmed by other workers (Eder & Telegdi 1952; Telegdi 1952). The latest result, which establishes that the cross-section has at least five resonances (Goward & Wilkins 1952*a*), still awaits independent confirmation in nuclear emulsion work, but has been confirmed by ionization-chamber measurements in progress at the Atomic Energy Research Establishment.

2. EXPERIMENTAL TECHNIQUES

2(a) Irradiation procedure

Bremsstrahlung irradiations were carried out with 3×1 in. Ilford plates (C2 and E1 emulsions) placed some 100 to 150 cm from the synchrotron target and carefully alined in the centre of the beam, giving reasonably uniform illumination of the whole emulsion volume. A thin absorber placed near the synchrotron target effectively removed soft electrons and γ -rays from the beam, and unnecessary fogging was avoided by wrapping the plates lightly and eliminating extraneous scattering material. In a few early irradiations the γ -ray beam impinged normally on the emulsion surface, but in the remainder a glancing angle of incidence of

about 2° was used; zero angle was avoided, to limit γ -ray attenuation and ionization build-up in the emulsion. Irradiation at glancing incidence permitted the direction of the beam in the plane of the emulsion to be accurately recorded by placing a thin flat piece of glass near the leading edge of each plate during irradiation; on development a narrow well-defined shadow was produced.

Irradiations with lithium γ -rays were carried out under the best geometrical conditions available, having regard to the low γ -ray intensities. Each 3×1 in. plate was arranged with a 1 in. edge about 4 cm from the target and with the 3 in. edges nearly parallel to the γ -rays, again giving glancing incidence.

2(b) Peak energy and intensity measurement

Satisfactory absolute calibrations of bremsstrahlung intensities and peak energies were not available until a late stage in the experiments. It was decided, therefore, to analyze all the results in a way (see § 4(b)) which did not require initial knowledge of intensity or peak energy, and to rely for absolute measurement on a limited number of recent carefully monitored irradiations using 33 MeV bremsstrahlung. In these special irradiations a standard aluminium-walled ionization chamber was used for intensity measurement in conjunction with an amplifier and recording ammeter. The absolute sensitivity of the chamber at n.t.p. for γ -rays up to 25 MeV has been calculated by Flowers, Lawson & Fossey (1952) with an estimated standard error of $\pm 7.5\%$, and extrapolation of their results to 33 MeV introduces negligible additional uncertainty. Corrections for deviations from n.t.p. and for γ -ray absorption by the plates both amounted to about 8%. Peak-energy calibration (not strictly necessary since it may be deduced from the star measurements) was effected by using a precision circuit to integrate the voltage induced in a small coil placed at the synchrotron target. The absolute value measured was 32.5 ± 0.5 MeV, comparing with a value 33.5 ± 1.0 MeV deduced from the stars.

A suitable bremsstrahlung dose for E1 emulsion, 200μ thick, at 33 MeV peak energy is 30 'R' units, or 10^{11} MeV/cm², producing about seventy $^{12}\text{C}(\gamma, 3\alpha)$ stars per cm² of plate. For a similar degree of background fog, C2 emulsion requires only 5 to 8 'R' units, while borax-loaded emulsion (0.04 g boron/cm³) requires about half that of a non-loaded emulsion of the same grade. The dose must be varied roughly in direct proportion to the peak energy. Considerably heavier doses can be given while still distinguishing events, but the doses quoted give reasonable conditions of low background fog and good proton tracks, allowing accurate track measurements to be made.

Lithium γ -ray doses were limited by available time and intensity, and were about 10^9 quanta/cm² (about 10^{10} MeV/cm²).

2(c) Processing

Emulsions were in general processed by standard methods, using amidol developer, with the aim of obtaining good discrimination between α -particles and protons, combined with a sufficiently low background fog to allow protons of at least 7 MeV energy to be detected in the E1 emulsions, or at least 10 MeV

energy in the C2 emulsions. Some refixing was useful for reducing background fog, but led to seriously impaired discrimination if carried to excess.

The borax-loaded emulsions were given additional pre-soaking in distilled water and required slightly less than the usual development time. Pre-soaking in sodium sulphate solution was occasionally necessary to prevent blistering.

2(d) Scanning and track measurement

The processed emulsions were scanned in swathes of about 100μ width, using $\times 500$ magnification, and all stars of three or more tracks were recorded. The detection efficiency achieved by the observers was checked at intervals by conventional coincidence methods, considerable areas of emulsion being scanned twice. $^{12}\text{C}(\gamma, 3\alpha)$ stars were generally detected with an efficiency of $(89 \pm 6)\%$ with the exposure and processing conditions described above. The coincidence statistics were not sufficient to reveal any dependence of detection efficiency on the size, orientation, etc., of the stars, although some variation appears to exist from other evidence (§ 4(a)).

Measurements of the tracks were made at a magnification of $\times 1400$. A detailed study of the accuracy achieved has been made elsewhere (Wilkins 1952), showing, for example, that each depth measurement (the mean of three readings) was subject to about $\pm 0.3\mu$ standard deviation. Errors in horizontal projections were certainly much less than the $\pm 0.9\mu$ range-straggling of the α -particles in the emulsions. Errors in azimuthal angles arose mainly from multiple scattering and irregular orientation of track grains, and amounted to about $\pm 8^\circ$ for a 1.0 MeV α -particle, decreasing rapidly for longer tracks.

The various measurement errors, and their relative importance, were not fully elucidated when the measurements were in progress. Most of the discrepancies between different observers clearly arose in making depth measurements, and the practical criterion adopted was that, on an average, α -particle (vector) momenta should be arrived at with equal accuracy in the horizontal and vertical directions (see § 3(b)).

The shrinkage factor of each emulsion was obtained by making direct measurements with a micrometer of the thickness of glass plus emulsion just before and just after exposure, and again after processing. The thickness of the processed emulsion was measured by microscope. Subsequent variations in emulsion thickness were detected by daily microscope observations. The emulsions irradiated with 70 MeV bremsstrahlung and with lithium γ -rays were exceptional, in that the initial thickness measurements were necessarily made at least some days before and after exposure. An adjustment amounting to a small percentage proved to be necessary to the shrinkage factor of the lithium γ -ray emulsions (Wilkins 1952).

2(e) Range-energy relationships

The range-energy relationships used were those developed by Wilkins (1951), which take account of borax and water content of the emulsions. Practical results obtained with them should be consistent to better than 2% in stopping power. The relationships for α -particles of low energy (< 1.5 MeV) were determined from

momentum-balance analysis of early $^{12}\text{C}(\gamma, 3\alpha)$ star measurements, and were found to depend on emulsion grain size and sensitivity, as well as on stopping power.

3. METHOD OF SELECTING $^{12}\text{C}(\gamma, 3\alpha)$ STARS

3(a) Types of star observed

Throughout the major part of the experiments all recorded stars contained entirely within the emulsion layer were measured unless they obviously arose from radioactive contamination, were obscured by an emulsion defect, or had ill-defined or badly scattered tracks. With the emulsions irradiated by 33 and 70 MeV bremsstrahlung, however, the experience gained by the observers was used to permit some rejection, without measurement, of stars of types it was not desired to study.

TABLE 1. SUMMARY OF EXPERIMENTAL DATA ON THREE-TRACK STARS

γ -ray source	emulsion	stars in emulsion			stars escaping			3 α stars	
		3 α	2 α p	others	3 α	2 α p	others	measured	identified $^{12}\text{C}(\gamma, 3\alpha)$
$^7\text{Li}(p, \gamma)^8\text{Be}$	E 1 (B)	559	173	—	39	23	—	529	470
21 MeV synchrotron	E 1 (B)	285	79	—	24	12	—	274	249
23 to 28 MeV synchrotron	E 1 (B)	1123	144	—	179	13	—	1033	905
	C 2 (B)	192	103	—	34	34	—	171	142
33 MeV synchrotron	E 1 (B)	410	133	3	81	31	—	360	286
	C 2 (B)	111	58	—	20	13	—	101	79
70 MeV synchrotron	E 1	738	213	21	184	59	12	468	326
	C 2	98	61	15	18	21	7	74	47

In column 2 the symbol (B) indicates borax loading in some of the emulsions used. The total number of stars in the table is 5325, including 2504 selected $^{12}\text{C}(\gamma, 3\alpha)$ stars.

Table 1 gives a detailed summary of all the three-track stars observed, other than obvious contamination stars, grouped according to the appearance of their tracks. Practically all these stars were consistent in appearance with either three α -particles (referred to as 3 α stars) or two α -particles and a proton (referred to as 2 α p stars), but may have included some ^3He or heavier nuclei and, occasionally, an obscured fourth track. In borax-loaded emulsions the 2 α p stars were mainly due to reaction (R8). The last two columns of the table show the number of 3 α stars measured, and the number finally selected as $^{12}\text{C}(\gamma, 3\alpha)$ stars with the aid of momentum-balance analysis.

3(b) Momentum-balance analysis

If the identities of the particles of a photodisintegration star are known, the particle energies E_r ($r = 1, 2, \dots$) in MeV and the momenta p_r in units of $(\text{MeV} \times \text{mass number})^{\frac{1}{2}}$ may be determined from the appropriate range-energy relationships. The momentum of the γ -ray in the same units is given by the relation

$$p_\gamma = 0.0232E_\gamma. \quad (2)$$

Defining a momentum vector, Δ , by the vector equation

$$\Delta = (\Sigma p_r) - p_\gamma, \quad (3)$$

conservation of momentum requires $\Delta = 0$. In practice, however, various factors combine to produce errors in the measured momenta, and a histogram of any component of Δ , resolved along some chosen direction, is of Gaussian form. The $^{12}\text{C}(\gamma, 3\alpha)$ measurements were sufficiently accurate to make the width of the Gaussian distribution approximately independent of the direction chosen, and it follows that a histogram of $|\Delta|$ should have Maxwellian form, i.e.

$$N(|\Delta|) d(|\Delta|) = (K |\Delta|)^2 \exp[-(K |\Delta|)^2] d(|\Delta|). \quad (4)$$

The expected Maxwellian distribution is confirmed by figure 1(a) which presents a ' $|\Delta|$ analysis' of all measured three-track stars produced by lithium γ -rays and by 20 MeV bremsstrahlung. All stars, whether of 3α or $2\alpha p$ appearance, were treated as $^{12}\text{C}(\gamma, 3\alpha)$ stars and the corresponding $|\Delta|$ values were calculated and plotted as shown. Most of the 3α stars are clearly resolved from the $2\alpha p$ stars and fall within the fitted Maxwellian distribution with maximum at $|\Delta| = 0.5$. Any 3α star giving $|\Delta|$ less than about 1.1 may be accepted with considerable certainty as $^{12}\text{C}(\gamma, 3\alpha)$. A small percentage of true $^{12}\text{C}(\gamma, 3\alpha)$ stars will, of course, give $|\Delta| \geq 1.1$, and correction must be made for them when estimating cross-section values.

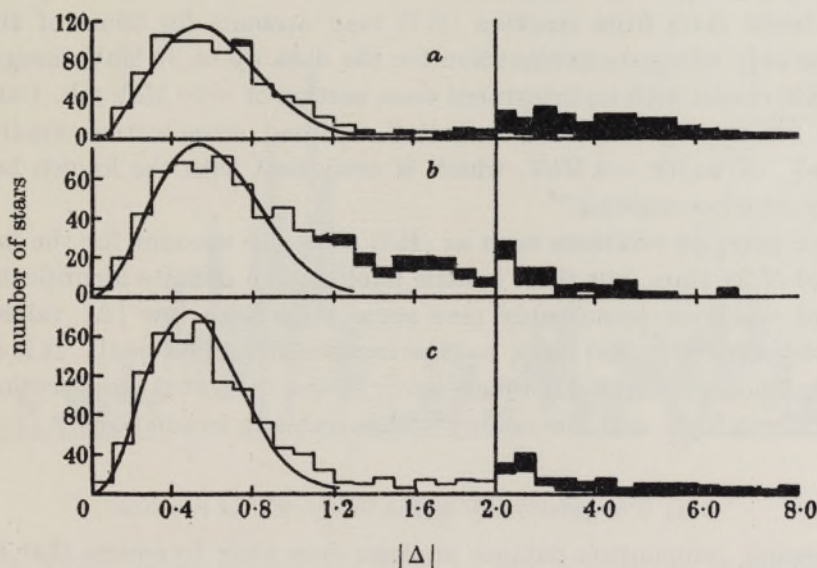


FIGURE 1. Momentum-balance analysis of three-track stars, all treated as $^{12}\text{C}(\gamma, 3\alpha)$ disintegrations. 3α stars are shown unshaded and $2\alpha p$ stars shaded. The fitted curves are of Maxwellian form. (a) Stars produced by lithium γ -rays and by 21 MeV bremsstrahlung. (b) Stars with $E_T < 9.7$ MeV produced by 24 to 70 MeV bremsstrahlung. (c) Stars with $E_T \geq 9.7$ MeV produced by 24 to 70 MeV bremsstrahlung.

The $|\Delta|$ distribution would be expected to vary in width for stars of different sizes, since the error in measuring momentum decreases (initially) with increasing momentum (Wilkins 1952). This tendency may be seen by comparing

figures 1*b* and 1*c*, which show the combined $|\Delta|$ statistics for the higher energy bremsstrahlung measurements. Figure 1*b* represents only small stars for which $E_\gamma < 17$ MeV, and figure 1*c* represents the larger stars for which $E_\gamma \geq 17$ MeV. All stars rejected without measurement would certainly have given $|\Delta| > 2.0$. For the small stars of figure 1*b* the distribution is similar to that in figure 1*a* except that the region $2 > |\Delta| \geq 1$ contains far more stars. These were clearly not caused by reaction (R 1) and should consequently be excluded. The large stars of figure 1*c* give the expected reduction in the width of the Maxwellian, combined with a smaller number of stars of doubtful identity near the tail of the Maxwellian curve, giving some indication that the 'background' stars in figure 1*b* were produced by reactions with a fairly high (effective) threshold energy. A single limiting $|\Delta|$ value is, on this evidence, unsuitable as a criterion for selecting stars, and the limiting $|\Delta|$ value chosen was varied between 0.8 and 1.1 according to the E_γ value and the emulsion type.

3(c) Evidence for the $^{13}\text{C}(\gamma, n) 3\alpha$ reaction

The background 3α stars mentioned in the preceding paragraph and shown in figure 1*b* are of sufficient importance to merit special consideration, since they cannot be attributed entirely to known reactions. The way in which the background varied as a function of the peak energy of the bremsstrahlung may be seen from table 1 by comparing the figures in the last two columns. Although confusion with four-track stars from reaction (R 7) may account for some of the background, the only adequate explanation for the data up to 33 MeV energy is that reaction (R 2) occurs with an integrated cross-section of ~ 20 MeV mb. Calculating E_γ values for appropriate stars indicated a broad cross-section maximum at $E_\gamma \sim 24$ MeV, of width ~ 4 MeV, which is consistent with the known behaviour of other (γ, n) cross-sections.

At higher energies reactions such as (R 3) probably account for the increasing background of 3α stars, but there is little likelihood of definite identification. The background reactions presumably give some stars with low $|\Delta|$ values, indistinguishable from $^{12}\text{C}(\gamma, 3\alpha)$ stars, but the number should be small. It is certainly so small that no significant differences occur in the $^{12}\text{C}(\gamma, 3\alpha)$ cross-section values as deduced from high- and low-energy bremsstrahlung irradiations.

3(d) The possibility of the $^{12}\text{C}(\gamma, \gamma') 3\alpha$ reaction

The foregoing momentum-balance analysis does little to ensure that the stars finally selected as $^{12}\text{C}(\gamma, 3\alpha)$ stars do not involve γ -rays emitted by reactions such as (R 5). To distinguish such processes a more sensitive analysis must be adopted, using a method described elsewhere (Goward & Wilkins 1951*a*).

First assuming that no γ -rays are emitted, the momentum of the incident γ -ray may be derived from equation (3) by resolving along the known direction of the γ -ray and assuming $\Delta = 0$. An experimental value of E_γ is thus obtained, using equation (2). The sum of the particle energies gives E_T , and hence equation (1) gives an experimental value of the reaction threshold E_B . The standard deviation on each E_B value obtained is rather large, about ± 15 MeV, but the mean of a

sufficient number of values should nevertheless be 7.28 MeV, with an appropriately reduced error.

If a γ -ray of energy E_a is emitted with random orientation, then an elementary extension of the above argument serves to show that the mean E_B value obtained will be $(7.28 + E_a)$ MeV.

Analysis of about half the selected stars of figure 1 gave a mean value of $E_B = 6.85 \pm 0.52$ MeV, which shows that appreciable contributions from the (γ, γ') process are unlikely in the selected stars. This conclusion finds support from the experiments using lithium γ -rays (see §§ 1 and 5), where the $^{12}\text{C}(\gamma, 3\alpha)$ stars found yield $(E_T + 7.28)$ values consistent with the known γ -ray energies.

4. RESULTS OBTAINED FROM SYNCHROTRON EXPERIMENTS

4(a) Distribution of energy release (E_T) in $^{12}\text{C}(\gamma, 3\alpha)$ stars

After selection of $^{12}\text{C}(\gamma, 3\alpha)$ stars by the method described, the first step towards obtaining cross-section values consisted in plotting histograms of the energy release $E_T (= \Sigma E_r)$ for the selected stars. The results are illustrated in figure 2, which combines the data from 33 and 70 MeV bremsstrahlung irradiations. A resolution in E_T of 1.0 MeV (total width at half maximum) or better would be expected, so fairly small intervals of 0.2 MeV have been used in plotting

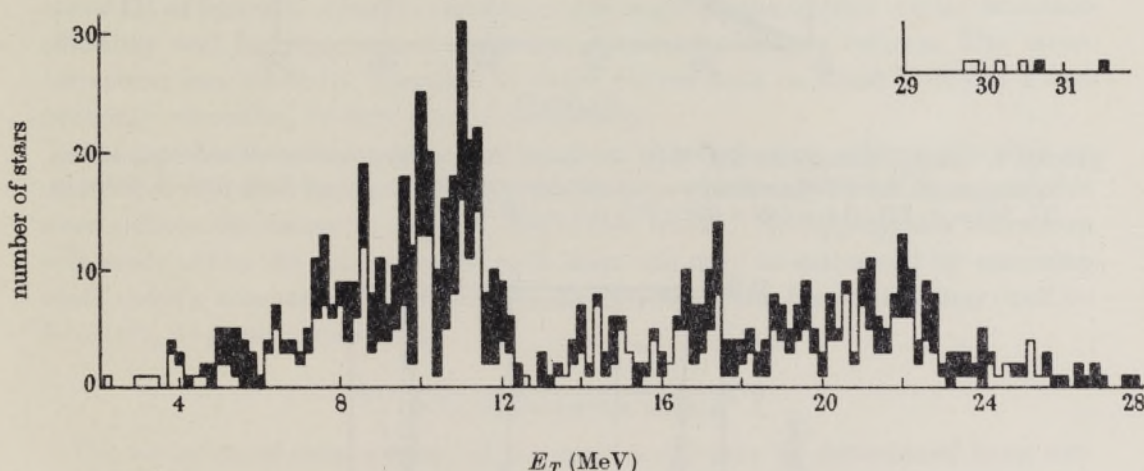


FIGURE 2. Energy-release histogram of $^{12}\text{C}(\gamma, 3\alpha)$ stars produced by 33 and 70 MeV bremsstrahlung. Shading indicates stars with steep tracks (average dip-angle $> 30^\circ$).

the histogram. The resolution may be improved by discarding stars with steeply dipping tracks, which are more affected by measurement errors, and the unshaded part of figure 2 includes only 'flat' stars, conveniently defined by the requirement $(\Sigma |\beta_r|) < 90^\circ$, where β_r ($r = 1, 2, 3$) denotes the angle of dip of a track. There is no evidence of systematic errors in shrinkage factor, which would produce a systematic difference between the E_T values of flat and steep stars.

The E_T histograms next required correction in order to arrive at the true total number of $^{12}\text{C}(\gamma, 3\alpha)$ stars formed in the emulsions. Correction for escape may be effected by means of the formula

$$F = \frac{(AB + BC + CA)}{4T}, \quad (5)$$

where F denotes the fraction of stars which have at least one track reaching a surface of an emulsion of thickness T . The significance of $(AB + BC + CA)$ is shown in the inset of figure 3, and the derivation of the formula is given in the appendix. It is valid only when the three tracks are coplanar, which is nearly enough true for $^{12}\text{C}(\gamma, 3\alpha)$ stars, and when AB , BC and CA are all $\leq T$. For any

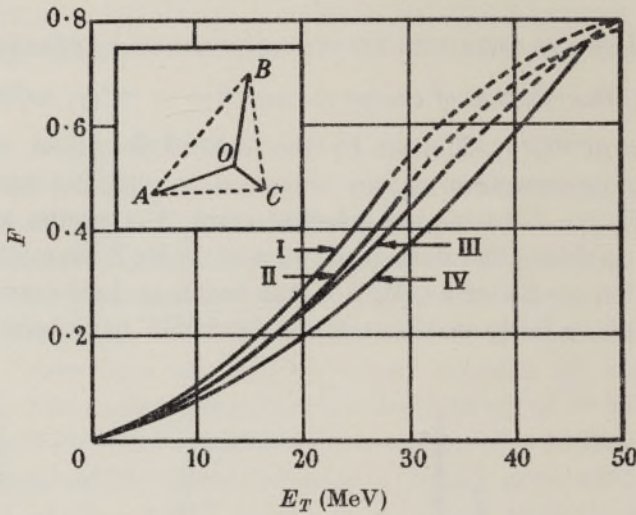


FIGURE 3. Escape corrections for $^{12}\text{C}(\gamma, 3\alpha)$ stars. The full-line curves are calculated from equation (5), for a 200μ emulsion, assuming geometries (see inset) such that: I, $OC = 0$; II, $BC = 0$; III, $OA = OB = 6OC$; IV, $OA = OB = OC$.

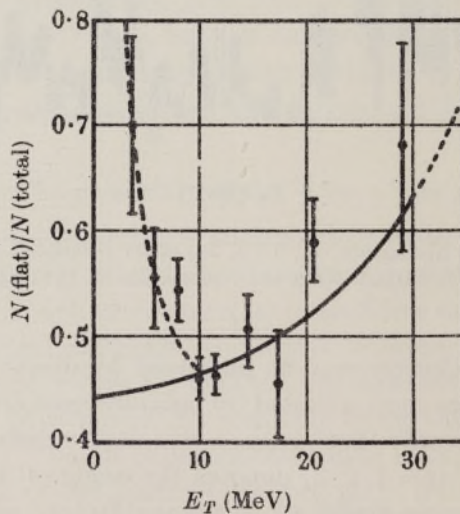


FIGURE 4. Proportion of $^{12}\text{C}(\gamma, 3\alpha)$ stars having $(\sum |\beta_r|) < 90^\circ$.

particular value of E_T a $^{12}\text{C}(\gamma, 3\alpha)$ star may have any one of an infinite number of geometries (although there is some correlation between E_T values and the types of star geometry most favoured) and a suitably averaged value of F is required. Figure 3 shows values of F calculated for $T = 200\mu$ and some particular star geometries, curve II, for example, applying to stars involving the ground state of ^8Be . Curve III represents a sufficiently accurate average value for general correction purposes.

The E_T histograms taken for correction included all stars for $E_T \geq 13$ MeV, but included only flat stars for $E_T < 13$ MeV. Restriction to flat stars at low energy was necessary, since statistical accuracy had a less critical effect on the histogram than had the resolution width, and also because a fall off in detection efficiency for small steep stars was revealed by means of figure 4, which shows the ratio $N(\text{flat})/N(\text{total})$ plotted as a function of E_T . $N(\text{flat})$ was defined as the number of selected stars with $(\Sigma|\beta_r|) < 90^\circ$, and $N(\text{total})$ as the total number of selected stars. Approximate calculation to allow for the greater proportion of steep stars (as compared with flat stars) which escape from the emulsion leads to the full-line curve in figure 4, assuming uniform detection efficiency and random orientation of the stars. Fall off in detection efficiency for small steep stars is clearly indicated by the experimental points for $E_T < 10$ MeV.

Complete correction of the E_T histogram thus proceeded in the following manner. First, for $E_T < 13$ MeV, $N(\text{flat})$ was corrected to $N(\text{total})$ using the calculated curve in figure 4. At all E_T values $N(\text{total})$ was then corrected for escape, using curve III of figure 3. Finally, allowance was made for the overall (89%) detection efficiency and for rejection of stars by momentum-balance criteria. The latter correction was made by reference to fitted curves such as those in figure 1 and generally amounted to only a small percentage.

One significant consideration omitted from this correction scheme was that an observer would tend to reject all $^{12}\text{C}(\gamma, 3\alpha)$ stars in which only two of the α -particles were sufficiently energetic to form observable tracks. No appropriate correction was made, since the proportion of such stars can only be estimated by assuming some specific mechanism for the $^{12}\text{C}(\gamma, 3\alpha)$ reaction; the proportion may well be 5 to 10% at some values of E_T .

4(b) Cross-section values

The variation of cross-section with γ -ray energy may be determined from corrected E_T histograms if the bremsstrahlung spectra and relative intensities used are known. Absolute measurement of intensity is necessary only to define an absolute cross-section scale. The form of spectrum assumed here was that given by Rossi & Greisen (1941) with suitable modifications of a few units per cent for absorbent material between target and emulsion. The E_T scale was converted to E_γ by means of equation (1), with $E_B = 7.28$ MeV.

The peak energies of the spectra used in all but the 70 MeV irradiations were determined by first calculating cross-section values from the 70 MeV irradiations alone. The quoted 70 MeV peak energy was subject to about ± 3 MeV uncertainty, but this has negligible effect on relative cross-section values at $E_\gamma < 50$ MeV. The

E_T histogram from a lower energy irradiation was then taken and the peak γ -ray energy determined as that which yielded cross-section variations in best agreement with the 70 MeV results. The error involved varied from about ± 0.3 to ± 1.0 MeV, according to the statistics available. The agreement between cross-section varia-

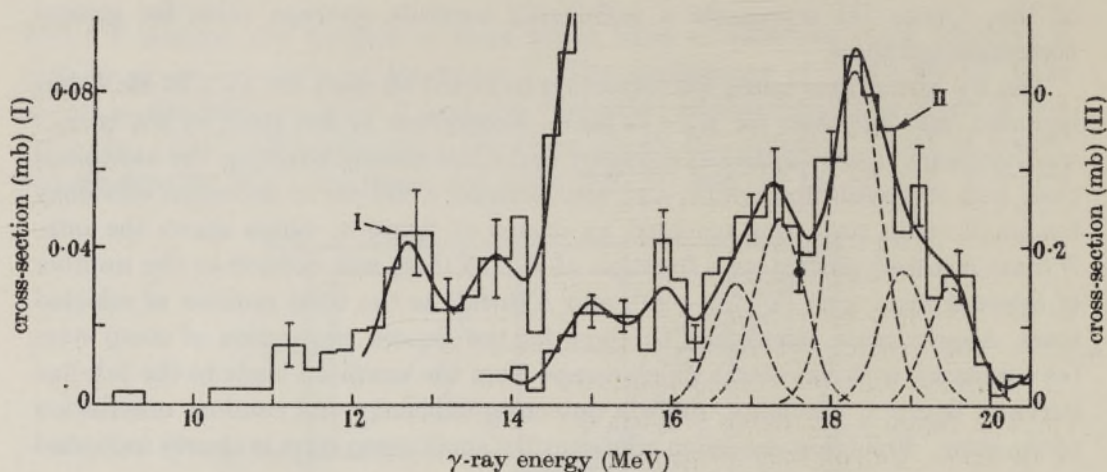


FIGURE 5. $^{12}\text{C}(\gamma, 3\alpha)$ cross-section for γ -ray energies less than 20.5 MeV (based on flat stars only).

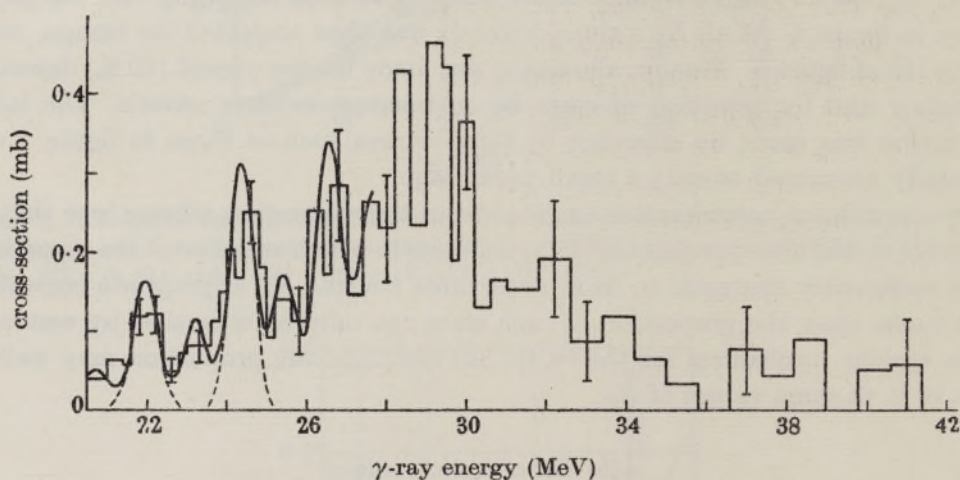


FIGURE 6. $^{12}\text{C}(\gamma, 3\alpha)$ cross-section for γ -ray energies above 20.5 MeV (based on total data).

tions obtained from the results of irradiations at different energies gave considerable confidence in the general form assumed for γ -ray spectra, and also gave some support for the absence of $^{12}\text{C}(\gamma, \gamma') 3\alpha$ stars amongst those selected.

The cross-section variation obtained from the combined results is shown in figures 5 and 6 in histogram form. The results of separate irradiations were normalized to give the same integrated cross-section for $14 \text{ MeV} \leq E_\gamma \leq 19 \text{ MeV}$, discarding all data within 1.5 MeV of the calculated spectral limit, since the form of the spectrum near the limit is not well known. The purely statistical uncertainties are indicated as standard deviations at intervals on the figures.

Calibration of the ordinate scales in absolute cross-section units was based only on special 33 MeV bremsstrahlung irradiations (see § 2(b)), assuming emulsion compositions from the data given by Wilkins (1951). (The cross-section units used are millibarns, where $1 \text{ mb} = 10^{-27} \text{ cm}^2$.) The greatest single sources of error were the ionization chamber calibration ($\pm 7.5\%$) and statistical errors in the number of stars ($\pm 6\%$), and a reasonable figure for the overall uncertainty in the absolute cross-section scales is $\pm 13\%$ standard deviation. The area under the histogram corresponds to an integrated cross-section of $1.21 \pm 0.16 \text{ MeV mb}$ for $E_\gamma < 20.5 \text{ MeV}$, and $2.8 \pm 0.4 \text{ MeV mb}$ for $20.5 \leq E_\gamma < 42 \text{ MeV}$. No stars were found with $E_\gamma \geq 42 \text{ MeV}$, indicating an upper limit of some 0.2 MeV mb for $42 \leq E_\gamma < 60 \text{ MeV}$.

5. RESULTS OBTAINED WITH LITHIUM γ -RAYS

5(a) Cross-section at 17.6 MeV

Figure 7 shows the histogram of energy-release (E_T) values for 470 $^{12}\text{C}(\gamma, 3\alpha)$ stars formed by $^7\text{Li}(p, \gamma)^8\text{Be}$ γ -rays. The γ -ray spectrum may be deduced from measurements published by Walker & McDaniel (1948) and from many related investigations (Hornyak, Lauritsen, Morrison & Fowler 1950). The principal

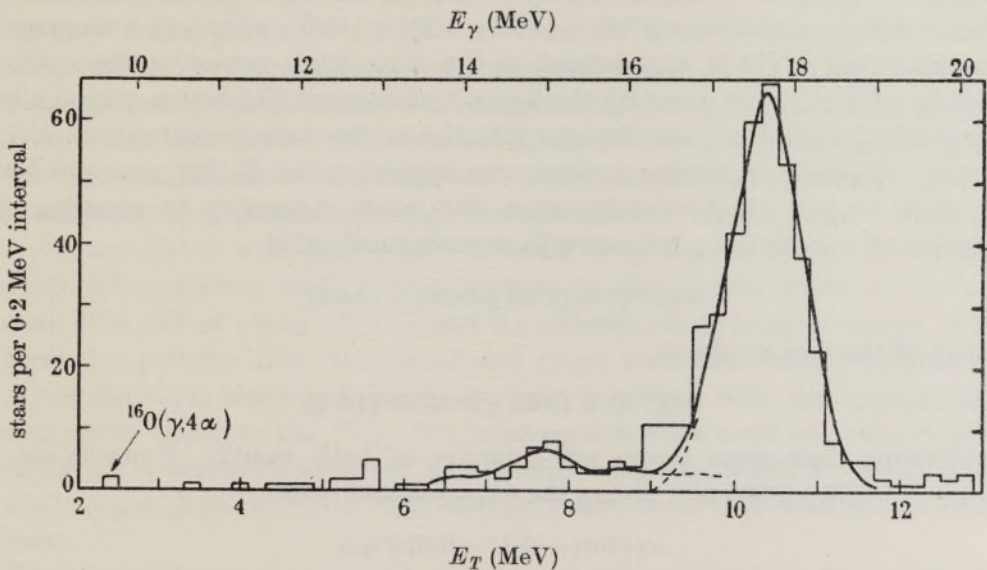


FIGURE 7. Energy release histogram for $^{12}\text{C}(\gamma, 3\alpha)$ stars produced by lithium γ -rays. The two smallest stars shown are probably $^{16}\text{O}(\gamma, 4\alpha)$, produced by 17.6 MeV quanta.

component is a narrow line of width 10 KeV and 17.6 MeV energy, and a second component about half (0.46 ± 0.04) as intense is centred at $14.6 \pm 0.2 \text{ MeV}$ energy. The second component is about 2 MeV wide and its exact form is not known, but a rough estimate may be made from the diagrams in Walker & McDaniel's paper. The corresponding E_T histogram of figure 7 is of already well-known form (e.g. Nabholz *et al.* 1952), but it is analyzed here mainly in order to study more closely the $^{12}\text{C}(\gamma, 3\alpha)$ cross-section variations near 17.6 MeV.

The analysis to be described primarily makes a comparison between (i) a value of the $^{12}\text{C}(\gamma, 3\alpha)$ cross-section at 17.6 MeV, $\sigma(17.6)$, derived from figure 7, and (ii) the value already indicated by the figure 5 histogram. As a result of limited experimental resolution the latter value, (ii), is strictly only a rather complex weighted mean of true cross-section values, taken over an interval of 1 or 2 MeV about 17.6 MeV. The former value, (i), however, is a mean over only 10 KeV or so, the width of the 17.6 MeV lithium γ -ray line. The comparison of values (i) and (ii) is made independent of measurements of the intensities of the bremsstrahlung or lithium γ -rays, and the significance of any discrepancy will thus be to reveal the presence of unresolved fine structure in the figure 5 histogram (this possible fine structure is discussed in §6).

The principle of the method is to assume the cross-section values of figure 5 to be correct for $E_\gamma < 17.6$ MeV (in the region of the wide 14.6 MeV lithium γ -ray line), but to treat $\sigma(17.6)$ as arbitrary. The E_T distribution of figure 7 may then be completely predicted from the known γ -ray spectrum except for the height of the peak at $E_T = 10.3$ MeV. Adjustment of this height to give agreement with the experimental histogram at once determines $\sigma(17.6)$.

The curve shown in figure 7 is the predicted E_T distribution adjusted for best fit to the observations, with full allowance for corrections discussed in §4(a). For a satisfactory fit it was necessary to assume an experimental resolution of 1.05 ± 0.10 MeV, and that $\sigma(17.6) = (1.72 \pm 0.32) \sigma'(14.6)$, where, as a convenient reference value, $\sigma'(14.6)$ was defined as the mean cross-section in the interval $13.6 \leq E_\gamma \leq 16.2$ MeV as given by the figure 5 histogram. The errors quoted allow for statistical limitations and for uncertainties in the various corrections and in the γ -ray spectrum. A similar analysis was applied to the E_T histogram of Nabolz *et al.* (1952), which contains over 2000 stars. Assuming an experimental resolution of 1.25 MeV a good curve fit was obtained, with

$$\sigma(17.6) = (1.58 \pm 0.23) \sigma'(14.6).$$

A mean of the two results is

$$\sigma(17.6) = (1.65 \pm 0.22) \sigma'(14.6),$$

remembering that some errors are common to both results. From figure 5, $\sigma'(14.6) = 0.103 \pm 0.008$ mb, giving the experimental point

$$\sigma(17.6) = 0.17 \pm 0.026 \text{ mb}$$

added to figure 5; its significance is discussed in §6.

5(b) Additional comments on the lithium γ -ray results

The overall $\pm 13\%$ uncertainty in the ordinate scales of figure 5 did not enter into the analysis in §5(a), since only a ratio, $\sigma(17.6)/\sigma'(14.6)$, was involved. Adding the $\pm 13\%$ determines the absolute value $\sigma(17.6) = 0.17 \pm 0.034$ mb. This value will be seen to be based on bremsstrahlung intensity measurements, rather than on intensity measurements of lithium γ -rays where poor geometry is usually unavoidable. Furthermore, the value is independent of the presence of any

lithium γ -rays outside the interval $13 \leq E_\gamma \leq 18$ MeV. For comparison with the results of direct determinations the cross-section value is best expressed in terms of σ (mean), the average cross-section for the 17.6 and 14.6 MeV γ -rays combined, for which the indirect method gives 0.140 ± 0.026 mb.

Direct determinations of σ (mean) have been reported by various workers (see §1 for references) and vary between 0.07 and 0.175 mb. Discrepancies probably arise from lack of attention to the corrections discussed in §4(a) and possibly from the presence of a γ -ray of energy ~ 12.5 MeV (Nabholz *et al.* 1951). Figure 7 is consistent with the presence of this γ -ray, since twelve stars are recorded with $E_T < 6$ MeV. According to the cross-section values of figure 5 the twelve stars indicate a γ -ray line of intensity 0.2 relative to the 17.6 MeV line, but it must be remembered that sharp cross-section resonances near 12.6 MeV would invalidate this estimate.

6. INTERPRETATION OF THE CROSS-SECTION RESULTS

Figures 5 and 6 clearly establish that the general trend of the $^{12}\text{C}(\gamma, 3\alpha)$ cross-section, as a function of E_γ , consists of two asymmetrical resonances with maxima at about 18.3 and 29.4 MeV, separated by a strong minimum at about 20.5 MeV. Closer inspection reveals that resonances at 21.9 and 24.3 MeV are also established beyond doubt. Attempts have been made to fit the complete histogram with a smooth curve having maxima at about 18.3 and 29.4 MeV only, but the fit was invariably unacceptable ($P \sim 0.0005$ in terms of a χ^2 test) over the interval $21 \leq E_\gamma \leq 26$ MeV. The additional experimental point at 17.6 MeV, derived in §5, also demands the existence of a resonance at about 17.3 MeV, although this resonance has been almost smoothed out by limited resolution in the histogram.

The five established cross-section resonances suggest rather strongly that the photodisintegration proceeds through excited states of ^{12}C , and that the resonances may be associated with particular ^{12}C levels or groups of levels. A compound nucleus interpretation finds further support in the general trend of the cross-section. The fall at about 19 MeV and the subsequent re-increase above 21 MeV suggest competition from the (γ, n) and (γ, p) reactions, whose cross-sections (e.g. Sagane 1951; Halpern & Mann 1951) are consistent with this interpretation. Attempts to calculate the $^{12}\text{C}(\gamma, 3\alpha)$ cross-section have used only direct photodisintegration theories and either an α -particle model (Telegdi & Zúnti 1950) or a shell model (Brinkworth & Skyrme 1951), and have met with rather limited success.

Recent studies of reactions such as $^{11}\text{B}(p, n)^{11}\text{C}$ and $^{11}\text{B}(d, n)^{12}\text{C}$ (reviewed by Ajzenburg & Lauritsen 1952) have revealed numerous ^{12}C levels spaced at roughly 0.5 MeV intervals. If excited levels of ^{12}C take part in the $^{12}\text{C}(\gamma, 3\alpha)$ reaction it is reasonable to inquire whether figures 5 and 6 can give any indication of levels at a closer spacing than the established 17.3, 18.3, 21.9, 24.3 and 29.4 MeV resonances. Several indications of such a fine structure are present (see also in figures 2 and 7), although they are for the most part within possible statistical fluctuations. Furthermore, attempts to fit a smooth curve in figure 5 between, say, 12 and 16.5 MeV lead to $P \sim 0.04$ in terms of a χ^2 test, and investigation of the basis of a fine structure is justified.

Before proceeding further it is necessary to estimate the experimental E_γ (or E_T) resolution. Once the resolution is known at any particular E_γ , its value at any other E_γ may be determined from the data of Wilkins (1952). A compromise has to be made between evidence from figures 5, 6 and 7 and from measurements of $^{16}\text{O}(\gamma, 4\alpha)$ stars observed in the same emulsions. Averaged over $^{12}\text{C}(\gamma, 3\alpha)$ stars of all orientations the resolution achieved may be assumed to be 1.0 MeV (width at half-amplitude) at $E_\gamma = 13$ MeV, improving to 0.75 MeV at $E_\gamma = 22$ MeV; for 'flat' stars the resolution is about 0.1 MeV better. At higher energies the combination of results from many different batches of emulsion probably caused a significant fall off in resolution.

To examine the consistency of figures 5 and 6 with the type of energy-level scheme currently recorded for ^{12}C , the extreme assumption has been made that the cross-section arises entirely from a series of levels of real width, small compared with the experimental resolution (say $\Gamma < 0.3$ MeV). The histogram is thereby visualized as a series of (overlapping) Gaussian curves, each of width equal to the known experimental resolution. The smallest required number of Gaussians was taken, and adjustments in height and position were made in order to fit the histogram, as shown. The component Gaussians used are partly indicated by dotted curves in the figures, and are detailed in table 2; the process was not continued above 27 MeV or below 12 MeV. Known levels of ^{12}C are also given in the table, and there is sufficient consistency to suggest that the analysis just described has some significance.

TABLE 2. NARROW RESONANCE ANALYSIS OF THE $^{12}\text{C}(\gamma, 3\alpha)$ CROSS-SECTION DATA

E_γ (MeV)	12.7	—	13.8	15.0	—	15.9
magnitude	0.040	—	0.035	0.115	—	0.113
known levels	12.8	13.3	(14.2)	15.1	(15.5)	16.1
E_γ (MeV)	16.8	17.3	18.3	18.9	19.5	20.7
magnitude	0.124	0.190	0.328	0.128	0.112	0.035
known levels	16.6	17.2	—	18.9	a	
E_γ (MeV)	—	21.9	23.2	24.3	25.4	26.5
magnitude	—	0.130	0.032	0.233	0.130	0.270
known levels	21.3	21.8	—	—	—	26.1

Magnitudes are in MeV mb units. In the third row, brackets denote a doubtful level and 'a' denotes a region in which several levels are known or suspected.

It is perhaps worth emphasizing that the analysis into a minimum number of Gaussians is a fairly critical and determinate process. The minimum number is itself closely fixed, since omission of any of those in table 2 would involve either leaving large numbers of stars unaccounted for (this point is well illustrated by figure 6), or arriving at a much more strongly peaked curve than the original histogram. The total heights of the Gaussians required in any one region is fixed by the area under the histogram. Finally (and most important), the positions are critical mainly because adjacent Gaussians usually intersect at points where their slopes are high. Position changes of 0.1 MeV alter the composite curve considerably.

Many other analyses and interpretations could of course be applied. For example, a smooth (double-peaked) continuum with superposed resonances could be considered, corresponding perhaps to a contribution from a direct photodisintegration, not involving a compound nucleus (Brinkworth & Skyrme 1951). Alternatively, a greater number of resonances could be assumed than in the foregoing treatment, or the assumed resonances could be assigned appreciable real widths. None of these interpretations can be profitably pursued at present, but there is little experimental evidence either for or against them.

Other evidence of γ -ray absorption into definite excited levels of ^{12}C is forthcoming from other experiments. An experiment now in progress at the Atomic Energy Research Establishment (Goward, Jones & Lasich), attempting to study the $^{12}\text{C}(\gamma, 3\alpha)$ cross-section with high resolution by an ionization-chamber method, gives preliminary results in reasonable agreement with table 2. The mechanism of the $^{12}\text{C}(\gamma, 3\alpha)$ reaction, as revealed, for example, by the angular distributions and correlations of the α -particles, shows significant variations over intervals < 1 MeV (Goward & Wilkins 1951c, and to be published). Again, R. Montalbetti *et al.*† have found sudden changes in the slope of the $^{12}\text{C}(\gamma, n)$ ^{11}C yield curve at energies consistent with table 2 over the region studied.

7. CONCLUSION

It has been shown that the variation of the $^{12}\text{C}(\gamma, 3\alpha)$ cross-section with γ -ray energy exhibits at least five 'resonances', situated at about 17.3, 18.3, 21.9, 24.3 and 29.4 MeV, with a particularly strong minimum occurring near 20.5 MeV. This behaviour is markedly at variance with existing theoretical calculations of the cross-section, which were based on direct photodisintegration theory, and strongly suggest that a well-defined $^{12}\text{C}^*$ compound nucleus is formed. The minimum at 20.5 MeV is then readily accounted for by (γ, n) and (γ, p) competition. The finer (and individually doubtful) details of the cross-section results are consistent with current knowledge of the level structure of ^{12}C (see table 2), giving increased support for the supposition that excited levels of ^{12}C participate in the reaction. The integrated $^{12}\text{C}(\gamma, 3\alpha)$ cross-section is 1.21 ± 0.16 MeV mb up to 20.5 MeV γ -ray energy, plus a further 2.8 ± 0.4 MeV mb up to 42 MeV. From 42 to 60 MeV only an upper limit of about 0.2 MeV mb can be assigned. The results have been shown to correspond to a cross-section of 0.140 ± 0.026 mb averaged over the 14.6 and 17.6 MeV lithium γ -rays.

A particularly valuable technique developed in the course of the work is the statistical 'momentum-balance' method of identifying stars produced by various reactions. A subsidiary result of its application has been to establish the reaction $^{13}\text{C}(\gamma, n) 3\alpha$.

It is a pleasure to acknowledge the generosity of Dr H. C. Pollock of the General Electric Co., Schenectady, U.S.A., who carried out the irradiations with 70 MeV bremsstrahlung, and of Dr D. H. Wilkinson of the Cavendish Laboratory, Cambridge, who provided facilities for the lithium γ -ray irradiations. We are indebted

† Private communication from L. Katz, University of Saskatchewan.

to Dr V. L. Telegdi, now at University of Chicago, U.S.A., for making known to us the experimental techniques used in his lithium γ -ray work and for collaborating in the preparation of an early report (Goward, Telegdi & Wilkins 1950). We are also indebted to many members of the synchrotron and nuclear emulsion group at the Atomic Energy Research Establishment for their indispensable assistance in irradiating, processing and searching emulsions and performing some of the routine computations. Miss E. Chellingworth, Miss P. Port and Miss M. Hart carried out some 50% of the track measurements. This work is published by kind permission of the Director, Atomic Energy Research Establishment, Harwell.

APPENDIX

A calculation of the fraction, f , of single tracks of length R which escape from an emulsion of thickness T has been given by Green & Livesey (1948), who prove the equations

$$f = \frac{R}{2T} \quad (\text{when } R \leq T), \quad (\text{A1})$$

$$f = \left(1 - \frac{2T}{R}\right) \quad (\text{when } R \geq T). \quad (\text{A2})$$

Equation (5) of the main text can be proved *ab initio* in a very similar way by first fixing the angle, ψ , between the planes of the three-track stars and the emulsion surface planes. Calculation of the escape fraction for $\psi = \text{constant}$ is fairly straightforward, after which integration over ψ leads at once to equation (5) for f .

An alternative proof may be based, as follows, directly on equation (A1). Referring to the inset of figure 3, OA , OB and OC denote the tracks of a coplanar star. Consider a random distribution of such stars in an emulsion of indefinite thickness, and note that these stars define equally random arrays of the lines AB , BC and CA . Now insert two parallel planes at spacing T , let the total number of stars originating between the two planes be N , and let a total number N_e of stars intersect one or other of the planes. By symmetry, only $\frac{1}{2}N_e$ of the latter stars will actually originate between the planes and thus

$$F = \frac{N_e}{2N}. \quad (\text{A3})$$

Each of the N_e intersecting stars defines two (and only two) of the corresponding lines, AB , BC and CA , which must also intersect the same plane as the star. The total number of intersections of AB , BC and CA with the two planes is thus $2N_e$. Now consider the random array of lines AB , and replace it by an identical array of single tracks of the same length, such as are referred to by equation (A1). N such tracks originate between the planes and, from equation (A1), a number $(AB) N/2T$ if these intersect one or other of the planes. It follows by symmetry that a total number $(AB) N/T$ of the complete array of lines AB intersect one or other of the planes, and by simple addition

$$\frac{N(AB + BC + CA)}{T} = 2N_e. \quad (\text{A4})$$

Using equation (A3), equation (5) follows at once.

It is useful to observe that in special cases when OA , OB and OC are collinear, equation (5) reduces to equation (A1), with R = overall length of the star. It may be shown that, under the same conditions but with $R \geq T$, equation (A2) is also applicable, enabling the dashed parts of curves I and II in figure 3 to be calculated.

Generalization of equation (5) to apply to any coplanar star with any number of tracks requires no modification of the above derivation, and leads to the following rule. Draw a polygon around the star, sufficient to enclose completely all its tracks, but having the least possible circumference, L . Then the fraction of stars which escape is given by

$$F = \frac{L}{4T}, \quad (\text{A5})$$

provided only that the greatest linear dimension of the polygon be $\leq T$.

REFERENCES

- Ajzenburg, F. & Lauristen, T. 1952 *Rev. Mod. Phys.* **24**, 321.
 Brinkworth, M. J., Goward, F. K. & Wilkins, J. J. 1952 *A.E.R.E. memorandum*, G/M130. London: H.M.S.O., code no. 70-674-0-94.
 Brinkworth, M. J. & Skyrme, T. H. R. 1951 *A.E.R.E. Rep.* T/R 802.
 Chastel, R. 1951 *C.R. Acad. Sci., Paris*, **233**, 1440.
 Eder, M. & Telegdi, V. L. 1952 *Helv. phys. acta*, **25**, 55.
 Flowers, B. H., Lawson, J. D. & Fossey, E. B. 1952 *Proc. Phys. Soc. B*, **65**, 286.
 Glätti, H., Seipel, O. & Stoll, P. 1952 *Helv. phys. acta*, **25**, 491.
 Goward, F. K., Telegdi, V. L. & Wilkins, J. J. 1950 *Proc. Phys. Soc. A*, **63**, 402.
 Goward, F. K., Titterton, E. W. & Wilkins, J. J. 1950 *Proc. Phys. Soc. A*, **63**, 172.
 Goward, F. K. & Wilkins, J. J. 1950 *Proc. Phys. Soc. A*, **63**, 662.
 Goward, F. K. & Wilkins, J. J. 1951a *Proc. Phys. Soc. A*, **64**, 93.
 Goward, F. K. & Wilkins, J. J. 1951b *Proc. Phys. Soc. A*, **64**, 201.
 Goward, F. K. & Wilkins, J. J. 1951c *A.E.R.E. memorandum*, G/M100. London: H.M.S.O., code no. 70-674-74.
 Goward, F. K. & Wilkins, J. J. 1952a *Proc. Phys. Soc. A*, **65**, 671.
 Goward, F. K. & Wilkins, J. J. 1952b *A.E.R.E. memorandum*, G/M127. London: H.M.S.O., code no. 70-674-0-65.
 Green, L. L. & Gibson, W. M. 1949 *Proc. Phys. Soc. A*, **62**, 296.
 Green, L. L. & Livesey, D. L. 1948 *Phil. Trans. A*, **241**, 323.
 Halpern, J. & Mann, A. M. 1951 *Phys. Rev.* **83**, 370.
 Hänni, H., Telegdi, V. L. & Zünti, W. 1948 *Helv. phys. acta*, **21**, 203.
 Hornyak, W. F., Lauritsen, T., Morrison, P. & Fowler, W. A. 1950 *Rev. Mod. Phys.* **22**, 291.
 Li, C. W., Whaling, W., Fowler, W. A. & Lauritsen, C. C. 1951 *Phys. Rev.* **83**, 512.
 Nabholz, H., Stoll, P. & Wäffler, H. 1951 *Phys. Rev.* **83**, 963.
 Nabholz, H., Stoll, P. & Wäffler, H. 1952 *Helv. phys. acta*, **23**, 858.
 Rossi, B. & Greisen, K. 1941 *Rev. Mod. Phys.* **13**, 240.
 Sagane, R. 1951 *Phys. Rev.* **84**, 587.
 Telegdi, V. L. 1952 *Phys. Rev.* **87**, 196.
 Telegdi, V. L. & Zünti, W. 1950 *Helv. phys. acta*, **23**, 745.
 Wäffler, H. & Younis, S. 1949 *Helv. phys. acta*, **22**, 614.
 Walker, R. L. & McDaniel, B. D. 1948 *Phys. Rev.* **74**, 315.
 Wilkins, J. J. 1951 *A.E.R.E. Rep.* G/R 664. London: H.M.S.O., code no. 70-674-0-73.
 Wilkins, J. J. 1952 *A.E.R.E. Rep.* G/R 1020. London: H.M.S.O., code no. 70-674-1-05.
 Wilkins, J. J. & Goward, F. K. 1950 *Proc. Phys. Soc. A*, **63**, 663.
 Wilkins, J. J. & Goward, F. K. 1951 *Proc. Phys. Soc. A*, **64**, 1056.